



37 **Abstract**

38

39 This paper aims to evaluate how varying degrees of land use/cover (LULC) changes across  
40 sub-catchments affects the flood peak at the catchment outlet. The Kona catchment, a part of  
41 the upper Damodar Basin in eastern India, was the study site. A HEC-HMS model was set up  
42 to simulate rainfall-runoff processes for two LULC scenarios three decades apart. Because of  
43 sparse data at the study site, we used the Natural Resource Conservation Service (NRCS)  
44 Curve Number (CN) approach to account for the effect of LULC and soil on the hydrologic  
45 response. Although a weak ( $r = 0.53$ ) but statistically significant positive linear correlation  
46 was found between sub-catchment wise LULC changes and the magnitude of flood peak at  
47 the catchment outlet, a number of sub-catchments showed marked deviations from this  
48 relationship. The varying timing of flow convergence at different stream orders due to the  
49 localised LULC changes makes it difficult to upscale the conventional land use and runoff  
50 relationship, evident at the plot scale, to a large basin. However, a simple modelling  
51 framework is provided based on easily accessible input data and a freely available and widely  
52 used hydrological model (HEC-HMS) to check the possible effect of LULC changes at a  
53 particular sub-catchment on the hydrograph at the basin outlet.

54

55

56

57

58

59

60

61

62

63

64

65 **Keywords:** Land use/cover change, peak discharge, NRCS CN, HEC-HMS, Sub-catchment,  
66 Flow Convergence Timing.

67

68

69

## 70 1 Introduction

71

72 Soil, topography and land cover are the most important factors that control rainfall-runoff  
73 processes at the scale of single flood events for river basins. As alterations in soil and  
74 topography are insignificant in the short term, changes in land cover are considered to be the  
75 key element in modifying rainfall-runoff processes (Miller et al., 2002). Land-use/land-cover  
76 (LULC) change and any consequent hydrological response have been prominent topics of  
77 research in recent years (Chen et al., 2009; Amini et al., 2011; Fox et al., 2012). With  
78 changing climate and the increasing frequency of flooding events across the world (Collins  
79 2009; Hurkmans et al. 2009; Xu et al. 2009), the effects of LULC changes on extreme runoff  
80 events are likely to draw more attention.

81

82 Wan and Yang (2007) concluded that anthropogenic land use change is one of the major  
83 drivers of an increased frequency of flooding incidents. At small spatial scales ( $< 2 \text{ km}^2$ )  
84 deforestation was reported to have strong correlation with increase in flooding (Bosch and  
85 Hewlett, 1982). However, the picture is less clear for larger catchments, where a number of  
86 studies have reported no significant change in flooding pattern with deforestation (Beschta et  
87 al., 2000; Andréassian, 2004) while others have observed even a negative trend in flood  
88 occurrence with reductions in forest cover (Hornbeck et al., 1997). Wei et al. (2008) reported  
89 an increase in the peak flow with deforestation but also observed that reforestation on the  
90 cleared land has limited effect on reducing the peak flow. Van Dijk et al. (2009) came to the  
91 conclusion that the empirical evidence and theoretical arguments for increased flood intensity  
92 with removal of forest are not very convincing. Shi et al. (2007) reported that high antecedent  
93 moisture conditions reduce the effect of increased urbanization on runoff in a small  $56 \text{ km}^2$   
94 catchment in Shenzhen, China.

95

96 A number of studies have attempted to analyse the impact of land-use change on storm runoff  
97 at the event scale (Chen et al., 2009; Ali et al., 2011; O'Donnell et al., 2011). LULC scenario-  
98 based studies have used past and present LULC states or radical LULC change scenarios in  
99 event-scale hydrological models to assess the hydrological response of catchments (Camorani  
100 et al., 2005; Olang and Furst, 2011). Chen et al. (2009) coupled a LULC scenario-generation  
101 model with a hydrological model and concluded that increasing urban areas led to increase in  
102 the total runoff volume and peak discharge of storm runoff events. Ali et al. (2011) conducted

103 an event-scale experiment in a predominantly urbanised catchment containing the city of  
104 Islamabad in Pakistan and had similar findings. It is noted that this type of study is generally  
105 restricted to small urban catchments, partly due to the easy availability of hydrological data  
106 near urban centres, the urgency of mitigating flooding problems in the centres of large  
107 population concentration and the general perception that expansion of built-up areas hampers  
108 infiltration and contribute a to the flood peak. It is not surprising that the finding of these  
109 studies coincide with the conventional wisdom that reduction in forest or increase in paved  
110 surface leads directly to increased runoff. An over-emphasis on the effect of afforestation and  
111 urbanization and lack of interest in examining the LULC changes in river basins with diverse  
112 LULC types have been the characteristics of recent research on the effect of land-cover  
113 change in flooding (Wan and Yang, 2007).

114 The contribution of streamflow from a specific land use is not uniformly proportional to the  
115 area of that land use and depends greatly on the location of that land use within the basin  
116 (Warburton et al., 2012). This study further showed that the streamflow response at the basin  
117 outlet is influenced by the spatial distribution of various land uses present in the entire  
118 catchment and the balancing or cancelling effect of those land uses. For example, where  
119 urbanization takes place in the upper sub-catchments, it leads to a disproportionately larger  
120 increase in the flood peak downstream (Amini et al. 2011). Human intervention by means of  
121 augmentation of channel capacity though improved channel management in the urban areas  
122 has been also found to act as a counterbalance to reduce the additional surface runoff  
123 generated by expanding urban area or reducing forests (Fox et al., 2012)

124

125 The primary application of findings from investigations dealing with LULC change and its  
126 effect on downstream flood peaks is in watershed management. Watershed management  
127 strategies often aim to identify the source area that generates a significant contribution to the  
128 downstream flood peak and implement remedial land use practices to reduce the runoff  
129 coefficient from this flood source area. As with the effects of LULC change on catchment  
130 hydrology, the effects of land management have been convincingly documented by studies  
131 involving small catchments (Bloschl et al., 2007; O'Connell et al., 2007). To be efficient,  
132 improvement of land use management practice should be based on a ranking of sub-  
133 catchments according to their contribution to downstream flood peaks.

134

135 Pattison and Lane (2012) reviewed this topic of possible relation between land-use change  
136 and possible downstream flood risk and pointed out that it is not uncommon to find an  
137 association between land-use change and streamflow behaviour at field and plot scales but it  
138 is quite challenging to upscale this effect to show similar hydrological responses for large  
139 catchments. Analysis and identification of the flood source area and its contribution at the  
140 cumulative basin outlet has been carried out with hydrologic modelling using the HEC-HMS  
141 model (Saghafian and Khosroshahi 2005; Roughani et al., 2007; Saghafian et al. 2008) and  
142 with statistical approaches involving rainfall and runoff data at the sub-catchment level  
143 (Pattison et al., 2008). Recently, Ewen et al. (2012) attempted to model the causal link  
144 between LULC changes at small scale to the flood hydrograph at the basin outlet by using  
145 reverse algorithmic differentiation and showed the sources of impact at the scale of small tiles  
146 that were used to decompose the model domain.

147

148 The statistical approach (Pattison et al., 2008) or the modelling approach (Ewen et al., 2012)  
149 are heavily dependent on a dense network of automatic rain and river gauging stations and  
150 are not possible to follow in a data scarce environment, which is typical in developing  
151 countries. Although a variety of hydrological models are available it is difficult to use them in  
152 data scarce environment such as India due to their requirement in terms of soil moisture and  
153 channel topography related data. The US Natural Resources Conservation Service (NRCS)  
154 curve number (CN) approach for runoff estimation is particularly suitable for applying in data  
155 scarce situations and has been widely used to estimate surface runoff in an accurate manner  
156 with limited data (Bhaduri et al, 2000; Mishra et al, 2003). The CN is an empirically derived  
157 dimensionless number that accounts for the complex relationship of land cover and soil and  
158 can be computed with widely available datasets such as satellite-derived LULC maps and  
159 small scale soil maps. Easy integration of remotely sensed LULC information has made the  
160 NRCS CN a popular choice among the scientific community for runoff estimation from the  
161 early days of remote sensing (Jackson et al., 1977; Slack and Welch 1980; Stuebe and  
162 Johnston 1990). There are numerous case studies that used remote sensing for deriving CN in  
163 order to estimate runoff at catchment scale with sparse data (*e.g.* Tiwari et al., 1991; Sharma  
164 and Singh, 1992; Amutha and Porchelvan, 2009). However, the strong seasonal pattern of  
165 land-use in monsoon climates has not been highlighted when comparing the hydrologic  
166 response of two land use scenarios observed over a period of few decades. Changing canopy  
167 cover and the proportion of cultivated land and other land covers may exert considerable  
168 control over rainfall-runoff processes.

169 The investigations to date have mostly dealt with the issue of LULC change across the  
170 catchment as a whole. However, as pointed out by Pattison et al. (2008), remedial land  
171 management practices are conceived and implemented at the sub-catchment scale. Although  
172 the modelling-based approach by Saghafian et al., (2008) and Roughani et al. (2007)  
173 attempted to identify the sub-catchments that have serious impact on the flood peak (flood  
174 source area) at the main catchment outlet, they did not assess how changes in LULC across  
175 the sub-catchment may change the location of the flood source area. There is a need for a  
176 systematic evaluation of sub-catchment wise LULC change and resultant changes in priority  
177 areas for implementing remedial land-use measures. LULC can change significantly in short  
178 periods, and the occurrence of LULC change in different parts of the catchment is likely to  
179 affect the flood peak at the catchment outlet in a complex manner.

180

181 This study is part of a broad investigation that deals with developing an adequate system for  
182 routing flood waves in the lower Damodar River in eastern India with freely available data  
183 and minimum ground survey (Sanyal et al., 2013) and modelling widespread floodplain  
184 inundation at a frequently flooded reach further downstream using low-cost high resolution  
185 terrain data (Sanyal et al., In-Press).

186

187 The objective of this study is to investigate (1) the effect of LULC change at sub-catchment  
188 level on the peak discharge at the catchment outlet during storm events, and (2) the interplay  
189 between sub-catchment position, LULC change and runoff. The findings of this paper have a  
190 direct implication on land-use management practices that are undertaken to reduce the peak  
191 inflow to reservoirs during storm events. The novel aspect of this investigation lies in the  
192 establishment of a direct link between sub-catchment scale LULC changes and their  
193 contribution to the flood peak at the basin outlet through semi-distributed rainfall-runoff  
194 modelling. In addition, this study also points out the typical challenges of modelling rainfall-  
195 runoff processes in data scarce environments and the required adaptations in methods to deal  
196 with this constraint.

197

## 198 2 Study Area

199

200 The Konar Reservoir is impounded by one of the four major dams in the upper catchment of  
201 the Damodar River in eastern India (Fig1). The catchment upstream of the reservoir is a

202 typical example of physiographic, drainage and LULC conditions in the upper Damodar  
 203 basin. A number of previous authors (e.g. Choudhury, 2011; Ghosh, 2011; Bhattacharyya,  
 204 1973) have argued that deforestation in the upper hilly and forested catchments in the upper  
 205 Damodar basin has increased both the runoff coefficient and flood peak, and has reduced the  
 206 capacity of the four reservoirs to moderate flood waves downstream. The catchment also  
 207 exemplifies the scarcity of required data for hydrological modelling, which is a typical  
 208 scenario in the developing countries. The catchment is drained by the Konar and Siwane  
 209 Rivers and is 998 km<sup>2</sup> in size. The topography is characterised by a dissected plateau region  
 210 with occasional hills. Elevation ranges from 402 to 934 m asl. The upland areas in the  
 211 catchment are mostly under forest cover while paddy cultivation during the monsoon season  
 212 is the dominant land use in the lower reaches. Rainfall has a strong seasonal pattern which is  
 213 heavily influenced by the southwest Indian monsoon. Torrential rain for a few hours per day  
 214 during the monsoon season (mid June to mid October) often leads to high magnitude floods  
 215 in this part of the Damodar Basin.

216

### 217 **3 Materials and Methods**

218

#### 219 *3.1 Generating curve numbers for two LULC scenarios*

220

221 The NRCS CN model is appropriate for use in data-sparse situations because the primary  
 222 model inputs are LULC and soil types that are easy to obtain from remote sensing and widely  
 223 available soil maps. The NRCS method of estimating runoff due to rainfall (NRCS, 1972) is  
 224 expressed in the following equations:

225

$$226 \quad Q = 0 \quad P \leq 0.2 S \quad (1)$$

227

$$228 \quad Q = (P - 0.2 S)^2 / (P + 0.8 S) \quad P \geq 0.2 S \quad (2)$$

229

230 where Q is the direct runoff depth (mm), P is the storm rainfall (mm), and S is the potential  
 231 maximum retention (mm). S is related to a dimensionless curve number, CN by:

232

$$233 \quad S = (254000 / CN) - 254 \quad (3)$$

234 In this method soil types are classified into four hydrological soil groups (A, B, C, and D)  
235 with increasing potential for generating runoff. Hydrological soil groups of any area can be  
236 identified by analysing soil texture. The method also considers the antecedent soil moisture  
237 condition by providing modified value for dry (AMCI) and wet (AMCIII) condition based on  
238 the preceding five days' daily rainfall.

239

240 In order to assess the impact of different land-cover scenarios on the peak flood discharge at  
241 the entry of the Konar Reservoir, two land-cover maps were generated from satellite imagery.  
242 A Landsat MSS image (79 m spatial resolution) from 27th October, 1976 and a Landsat TM  
243 image (30 m spatial resolution) from 2nd November, 2004 were used for generating two  
244 LULC maps. These two dates were chosen as this is the largest time span that was possible to  
245 capture with due considerations to the availability of cloud-free images at the final stage of  
246 the southwest monsoon season when the flood events considered took place.

247

248 Unsupervised classification was used to classify each image into 30 spectral classes. In the  
249 next step, the spectral classes were compared with a high resolution panchromatic Corona  
250 satellite image from 21st November, 1973 and a topographic map (1:50,000 scale) from the  
251 Survey of India (Map No. 73 E/5) which was surveyed in 1978-79. Similar classes were  
252 combined appropriately to create a land-cover map for 1976. High resolution QuickBird  
253 images available in GoogleEarth for 15th November, 2004 was utilised for the same purpose  
254 in order to classify the Landsat TM image of 2004. Finally we generated two LULC maps  
255 with following classes: 1) water body, 2) rocky waste, 3) urban area, 4) paddy field, 5) shrub,  
256 6) open forest, and 7) dense forest. There is a potential problem in comparing LULC changes  
257 from pixel to pixel between the two time periods because of the use of different sensors for  
258 acquiring the two images. However, Landsat MSS and TM data have been successfully used  
259 with unsupervised classification for identifying changes of broad land cover categories in  
260 Africa (Brink and Eva, 2009). The spectral resolutions of Landsat MSS and TM for Band 1, 2,  
261 3 and 4 are quite close and we only attempted to identify the broad land cover classes that are  
262 identifiable in the coarse resolution Landsat MSS images. Post-classification comparison of  
263 the LULC maps for the two time periods is likely to eliminate most of the discrepancies  
264 arising from the use of different sensors and spatial resolution. Due to the limitation of the  
265 spatial and spectral resolution of the available satellite imagery, identifying land-cover  
266 classes for which a CN value is available in standard lookup tables was not always possible  
267 and an adjustment of the CN table was necessary to get optimal runoff estimates using the



268 NRCS-CN approach (Kumar et al., 1991). We used the CN lookup table compiled by  
269 Tripathi et al. (2002) for land-use and soil texture classes in the Nagwan sub-catchment, a  
270 part of the Konar Reservoir catchment, except that the CN value for paddy fields was taken  
271 from Shi et al. (2007); the table in Tripathi et al. (2002) classified the paddy fields as upland  
272 and lowland paddy, but it was not possible to distinguish these in our land-cover  
273 classification. Hydrologic soil groups of the study area were determined by consulting the  
274 composition and texture of the soil types obtained from the soil maps of National Bureau of  
275 Soil Survey and Land Use Planning, India (NBSS&LUP). The land-cover maps and  
276 hydrologic soil groups map were combined using the lookup table in GIS to create CN maps  
277 for 1976 and 2004.

278

### 279 *3.2 Setting up the rainfall-runoff model*

280

281 The HEC-HMS modelling suite was chosen for simulating the rainfall-runoff process, as this  
282 package has a host of modelling options for computing the runoff hydrograph for each sub-  
283 basin and routing it through river reaches at the basin outlet (Beighley and Moglen, 2003).  
284 HEC-HMS has the option of using the NRCS CN method for computing direct runoff volume  
285 for a given rainfall event, which is a popular modelling choice for application in the data  
286 scarce environment (Olang and Furst, 2011; Candela et al., 2012; Du et al., 2012; Jia and  
287 Wan, 2011; Amini et al., 2011). The model has a GIS pre-processor known as HEC-GeoHMS  
288 which was used for extracting and integrating GIS data such as DEM, LULC and soil maps  
289 into the hydrological model.

290

291 A total of 124 sub-catchments were delineated from the SRTM DEM in the Konar catchment  
292 during the pre-processing stage in HEC-GeoHMS. The streams were vectorised from the  
293 topographic maps of the study area for use as a reference for guiding the automated sub-  
294 catchment delineation from the SRTM DEM. Das et al. (1992) used Strahler's stream  
295 ordering technique to identify the optimal basin size for NRCS-CN-based estimation of  
296 runoff volume for part of the upper Damodar River basin and this principle was used in our  
297 study. After filling the sinks a threshold contributing area of 5 km<sup>2</sup> was found suitable to  
298 delineate the streams that in general match the 2nd-order streams in the topographic maps.  
299 Due to the coarse nature of the SRTM DEM we could not automatically extract the 1st order  
300 streams as found in the topographic maps.

301

302 Sub-daily rainfall is an essential input for simulating storm runoff, particularly in tropical  
303 region where high intensity rainfall for a few hours often leads to flooding. We obtained  
304 rainfall data at 1 hour intervals for a storm event lasting from 11 to 12 October, 1973 from an  
305 autographic rain gauge located in Hazaribagh Town (Fig1). The data are supplied by the  
306 Indian Meteorological Department (IMD). In order to validate the accuracy of the model for  
307 the 2004 land cover scenario we used a storm rainfall event from 8-10 October, 2003, which  
308 was estimated by the 3B42 V6 product of the Tropical Rainfall Measuring Mission (Huffman  
309 et al., 2007). No gauged sub-daily rainfall data was available after 1976 as the autographic  
310 rainfall station has been defunct since then. The October, 2003 event was deemed most  
311 appropriate as the CN values for 2004 derived from a Landat TM image acquired on 2nd  
312 November reflected a land cover that is very similar to the prevailing LULC situation when  
313 the storm event of 2003 took place. It has been reported that TRMM data frequently do not  
314 match with *in situ* observations. For this reason, the area averaged 3-hourly 3B42 V6 TRMM  
315 data for the Konar catchment were summed into daily totals and compared with the daily  
316 rainfall product of the Indian Meteorological Department (Rajeevan and Bhate, 2008) which  
317 is derived from rain gauges and supplied in 0.5 degree gridded format. We found that the  
318 TRMM records for the 3 days (8-10 October, 2003) was only 3.7% higher than the IMD  
319 figures. After considering the preceding rainfall of last 5 days for the 1973 and 2003 events  
320 from the daily rainfall products of IMD we decided that the antecedent moisture condition  
321 was normal (AMCII) (35-53 mm) for the 1973 event but it was dry (AMCI) (> 35 mm) for  
322 the 2003 event. Hence, the normal CN values for the 2004 land cover scenario were  
323 converted to AMCI using the formula proposed by Mishra et al. (2008):

324

$$325 \quad CN_I = CN_{II} / (2.2754 - 0.012754 CN_{II}) \quad (4)$$

326

327 As four TRMM tiles cut across the Konar catchment, we downloaded and stacked 3-hourly  
328 gridded TRMM data for those four tiles for the storm period and extracted the pixel data into  
329 a time series. In the next step, four artificial rain gauges were created in HEC-HMS for the  
330 NW, NE, SW and SE portions of the Konar catchment and the gauges were populated with  
331 the extracted pixel values of the corresponding TRMM grid. In this way we managed to use  
332 quasi-distributed rainfall data into HEC-HMS for simulating the 2003 storm event.

333

334 The total rainfall received during the 1973 event was 156.7 mm where 132.3 mm was  
335 received on 12 October, 1973. The rainfall amount for the 2003 event, as derived from the

336 spatial average of the TRMM data was 176 mm from 07 to 09 October, 2003. 80.63 mm of  
337 rainfall was received in 12 hours between 08 to 09 October, 2003.

338

339 We have no access to long-term time-series of observed daily discharge data at the model  
340 outlet (Inflow to Konar Reservoir) for computing return periods of the two storm events that  
341 were considered for the present study. However, Fig 2 provides the general characteristics of  
342 the 1973 and 2003 storm events relative to few other major storm events for which daily  
343 discharge data at the model outlet is available with us. From this limited available data we  
344 may assume that that both events under consideration in this study are average major storm  
345 events in the Konar catchment.

346

347 The highest temporal resolution of available rainfall data was 1 hour (1973 event).  
348 Considering the small lag times of the smaller sub-catchments in the Konar catchment, it was  
349 found unrealistic to run the model at 1 or 3 hour time step. A five minute time step was  
350 selected for both models and consequently, the rainfall data for 1973 and 2003 were  
351 proportionately disaggregated into five minutes interval to match the modelling time step.  
352 Since only one functional rain gage (Hazaribagh Town) capable of recording rainfall at a sub-  
353 daily interval (1 hour) was available for the 1973 event it was used and we had to assume  
354 uniformly distributed rainfall.

355 TRMM 3-hour interval rainfall estimates are available for a spatial resolution of 0.25 degrees.  
356 Konar Basin was almost uniformly subdivided into four such TRMM grids. It was  
357 recognised that the 2003 TRMM data is almost certainly of inferior quality than the hourly  
358 rain gauge data that was available for the 1973 event . Deriving the mean of four  
359 corresponding TRMM grids would further deteriorate the quality of the rainfall input for the  
360 2004 event. In order to avoid this deterioration in the quality of the input rainfall we did not  
361 used a spatially uniform rainfall input similar to the 1973 event and this factor should be  
362 given due consideration for comparing the results of the two simulations. However, we would  
363 like to emphasise that the aim of presenting the rainfall event of 2003 with the LULC  
364 condition of 2004 was to only to establish that the model is capable of simulating the rainfall-  
365 runoff process in the Konar Basin for different rainfall and LULC conditions with reasonable  
366 accuracy.

367

368 The NRSC unit hydrograph lag method was used for computing the basin lag which is  
369 necessary for transforming the excess rainfall (or direct runoff volume) into runoff into the  
370 channels. Finally, the Muskingum-Cunge flow routing model was employed to route the flow  
371 through the channels to the outlet. Initially the model was run with the hourly rainfall of 11-  
372 12 October, 1973 and the CN values (AMCII) derived from the 1976 land cover map and the  
373 results were compared with the available daily runoff volume at the entry point of the Konar  
374 Reservoir (basin outlet). In the next step, the model was run with the 3-hourly TRMM rainfall  
375 of 8-10 October, 2003 with the CN values (AMCI) of 2004 and the hydrograph in terms of  
376 daily runoff volume was compared with the observed data. Following Knebl et al. (2005) and  
377 McColl and Agget (2007) it was anticipated that evapotranspiration losses would be  
378 negligible as the interest of this study is in high intensity monsoon storms that lead to  
379 flooding. Since our model only simulated the direct runoff, we derived the base flow  
380 component from the observed daily discharge data graphically by joining the points of  
381 inflection of the rising and falling limb of the hydrograph and eliminated this flow component  
382 in order to make the observed and modelled figures comparable.

383

384 The relationship between changing LULC patterns in the sub-catchments of the Konar  
385 catchment and the peak rate of discharge at the reservoir inlet was assessed by computing the  
386 unit flood response (Saghafian and Khosroshahi, 2005) of each of the 124 sub-catchments for  
387 the LULC scenarios of 1976 and 2004. The unit flood response approach can be used to  
388 standardise the contributions of sub-catchments to the peak flow. With changing land use, the  
389 unit flood response of various sub-catchments within a catchment is likely to change. The  
390 storm event of 11-12 October, 1973 was used as the meteorological input in both scenarios.  
391 The unit flood response approach ranks each sub-catchment on the basis of their contribution  
392 to the flood generation at the basin outlet and is expressed by

393

$$394 \quad f = \Delta Q_p / A \quad (2)$$

395

396 where  $f$  ( $\text{m}^3\text{s}^{-1}\text{km}^{-2}$ ) is unit area flood index,  $\Delta Q_p$  is the amount of decrease in peak discharge  
397 at the basin outlet due to elimination of a particular sub-catchment ( $\text{m}^3/\text{s}$ ), and  $A$  is the sub-  
398 catchment area ( $\text{km}^2$ ). A version of the HEC-HMS model containing all basin components  
399 was saved. In order to compute  $f$  for a particular sub-catchment we disabled that sub-  
400 catchment while keeping the connectivity of the streams intact for the entire model. In the  
401 next step, this model was run (without the contribution of the disabled sub-catchment) and

402 the f value for that particular sub-catchment was derived by subtracting the peak flow of the  
403 modified model from the peak flow of the model that incorporates all the sub-catchments.

404

## 405 **4 Results**

406

407 The changes in LULC for the entire Konar catchment from 1976 to 2004 (Fig 3) show  
408 considerable increase in rocky waste and decreases in the areas under paddy cultivation and  
409 open forest (Table 1).

410

411 Between 1976 and 2004 a substantial percentage of the total area in the Konar catchment  
412 changed in LULC from paddy to rocky waste, paddy to shrub, open forest to shrub and paddy  
413 to urban (Fig 4). The comparison of the simulated rainfall runoff event of October 1973 with  
414 the LULC situation prevailing in 1976 (Fig 5) reveals a good match between the observed  
415 and simulated daily streamflow volume. The association between the modelled and observed  
416 daily surface runoff figures for the 2004 LULC situation using the 2003 TRMM rainfall  
417 estimates (Fig 6) also shows a good match.

418

419 When considering the effect of LULC change in the entire Konar catchment on the peak  
420 discharge for the 1973 storm event at the reservoir inlet we found that, for the 1976 LULC  
421 scenario the peak discharge was 1023.3 m<sup>3</sup>/s occurring on 12th October at 20:10, while for  
422 the 2004 LULC scenario the peak discharge increased to 1194.7 m<sup>3</sup>/s and the time to peak  
423 was decreased by 1 hour and 10 minutes. After ranking the sub-catchments according to the  
424 unit flood response computed with the rainfall event of 1973 and LULC scenarios of 1976  
425 and 2004 (Fig 7), we found that in spite of significant LULC change between 1976 and 2004  
426 (Fig 3) there was little change in the ranking.

427

428 The spatial patterns of the percentage change in the CN values (Fig 8a), a proxy for the  
429 change in the combined effect of the soil and LULC, and the unit flood response between  
430 1976 and 2004 LULC scenario (Fig 8b) did show some degree of agreement; sub-catchments  
431 showing a higher percentage change in CN values (i.e. change in LULC) in the  
432 predominately forested area in the south and near the main stream of the Konar River tend to  
433 show an increase in their unit flood response values between the 1976 and 2004 LULC  
434 scenarios. The location of the LULC change in terms of the distance from the outlet may

435 have a negative impact on the intensity of the consequent percentage change in unit flood  
436 response. In order to test this, an attempt was made to assess if the distance from the sub-  
437 catchment centroid to the outlet, measured along the connecting stream network, had a  
438 statistically significant negative relationship with percentage change in unit flood response.  
439 However, no statistically significant relationship could be established.

440

441 Finally, a weak positive linear correlation was found (Pearson's correlation coefficient ( $r$ ) of  
442 0.53 ( $p < 0.01$ ) between the sub-catchment percentage change in unit flood response (1976 -  
443 2004) and curve number (CN) values (Fig 9a). Three clusters of sub-catchments showed  
444 marked deviations from the overall positive trend between the two variables. Cluster 1  
445 consists of sub-catchments with a large increase in CN values from 1976 to 2004 and a  
446 disproportionately large increase in the unit flood response. Cluster 2 consists of sub-  
447 catchments with a moderately high percentage increase in the CN values but a negative  
448 change in unit flood response values. Cluster 3 includes sub-catchments with small increases  
449 in CN values but large increases in unit flood response. In order to reveal any apparent  
450 geomorphological reason for these deviations from the overall trend we mapped the sub-  
451 catchments falling in the three aforementioned clusters which did not reveal an overall  
452 relationship between the location of LULC changes and proximity to higher order streams or  
453 the basin outlet (Fig 9b).

454

455 As we could not establish a relationship between the proximity of LULC change to the outlet  
456 or a higher order trunk stream and the peak discharge at the catchment outlet due to paucity  
457 of data, we tested the influence of timing effect of flow convergence at the sub-catchment  
458 level following the general argument of Pattison et al. (2008). In HEC-HMS, a single sub-  
459 catchment (with identifier W2080) and a junction (identifier J425) were selected as an  
460 example of a disproportionate rise in unit flood response (UFR) caused by moderate increase  
461 in CN value (LULC change towards more runoff producing LULC). (Fig 9a). On the other  
462 hand, sub-catchment W2510 and Junction J328 were chosen as an example of the general  
463 positive linear correlation between unit flood response and CN change between 1976 and  
464 2004 LULC conditions (Fig 9a). The location of these sub-catchments can be found in Fig 10.

465

466 W2080 demonstrated a 93 percent change in the unit flood response for only 2.03 percent  
467 change in the CN values from 1976 to 2004. The simulated hydrographs for W2080 showed  
468 little difference in the direct runoff pattern for the LULC conditions of 1976 and 2004 alone

469 (Fig. 11). Under the LULC conditions of 2004, Junction J425, the confluence of runoff  
470 generated from W2080 and the Konar River, experienced a peak discharge of 484.3 m<sup>3</sup>/s at  
471 15:35 on 12 October. At that time, the discharge from W2080 was 4.40 m<sup>3</sup>/s which was  
472 22.9 % of its peak discharge (19.2 m<sup>3</sup>/s) (Fig 11). The contribution of W2080 to the  
473 combined discharge at 15:35 on 12th October was thus 0.90 %. Using the LULC conditions  
474 of 1976, when the discharge from W2080 merged with the Konar River during the peak  
475 outflow at J425 on 12 October, 16:35 (1 hour later than the 2004 LULC scenario) the  
476 combined discharge at J425 was 383.8 m<sup>3</sup>/s and the contribution from W2080 was 2.1 m<sup>3</sup>/s  
477 (0.55% of the total) which was only 11.5% of its peak discharge of 18.3 m<sup>3</sup>/s (Fig 11). This  
478 example illustrates that with only a 2.3 percent increase in the CN value from 1976 to 2004,  
479 the contribution of the sub-catchment W2080 to the combined flow of a vast contributing  
480 area almost doubled (0.55% to 0.90%).

481

482 Sub-catchment W2510 revealed a different picture at Junction J328, where the runoff from  
483 the sub-catchment converged with the Konar River. Under the 2004 LULC conditions J328  
484 experienced a combined peak discharge of 280.7 m<sup>3</sup>/s at 15:15 on 12th October. At that time  
485 the discharge from W2510 was 7.8 m<sup>3</sup>/s, which was 2.77% of the combined discharge and  
486 65.54 % of the peak discharge of W2510 (11.9 m<sup>3</sup>/s) (Fig 12). For the LULC conditions of  
487 1976, the runoff from W2510 merged with the peak discharge at J328 on 15:45 (30 minutes  
488 later than 2004 LULC case) at a rate of 6.1 m<sup>3</sup>/s, which was 2.42 % of the combined peak  
489 flow of 251.7 m<sup>3</sup>/s. The runoff from W2510 at that time was 70.11% of its peak discharge  
490 (8.7 m<sup>3</sup>/s) (Fig 12). This test case illustrated that for a moderate 11% increase in the CN value  
491 from 1976 to 2004 LULC conditions the contribution of W2510 during the peak flow at  
492 Junction J328 increased from only 2.42% to 2.77%, which is in line with the overall trend in  
493 Fig 6.8.

494

## 495 **5 Discussion**

496

497 If we consider the effect of overall LULC changes in the Konar catchment to the flood peak  
498 at the catchment outlet, it becomes evident that a general increase in the higher runoff  
499 producing LULC classes resulted in higher peak discharge and shortened the time to peak.  
500 However, when investigating the sub-catchment-wise local LULC change and its influence  
501 over the peak discharge at the catchment outlet a complex relationship began to emerge.

502 When the location of the sub-catchments showing marked deviation from the overall trend  
503 was mapped (Fig 9) we could not find a convincing reason for their unusual hydrologic  
504 response, For example, two of the predominantly deforested sub-catchments in cluster 1 (see  
505 Fig 3 and 9b) were found to be near the trunk stream, which may explain their rapid reaction  
506 in terms of increase in percentage unit flood response; however, the other two sub-catchments  
507 in the same cluster that are located at the farthest point from the outlet did not have any  
508 apparent physical explanation based on the distance from the outlet or proximity to a stream  
509 of very high stream order. Nothing could be established about the negative reaction of the  
510 sub-catchments in cluster 2 to their contribution to the peak discharge at the outlet. The sub-  
511 catchments in cluster 3 were found to be adjacent to each other and located at a consistent  
512 position near the main stream (Fig 9) which may partially explain the spike in their  
513 percentage increase in the unit flood response caused by moderate positive percentage change  
514 in CN values.

515

516 Although an overall statistically significant positive relationship was found between the  
517 changes in LULC at the sub-catchment scale and their impact on the basin flood peak, the  
518 pattern was altered by other factors. Increments of 2.03% and 11% in the CN values of sub-  
519 catchment W2080 and W2510 between 1976 and 2004 resulted in expected changes in their  
520 surface runoff hydrographs (Fig 11 and 12). However, during the peak discharge at the  
521 junctions where the runoff from these two sub-catchments flows into the Konar River, their  
522 contribution to the combined flow differed markedly. Pattison and Lane (2012) highlighted  
523 the important role played by the timing of extreme rainfall events at different parts of the  
524 catchment and the consequent hydrological response. In addition, they also pointed out that  
525 the structure of the basin also determines the convergence of hillslope and channel flow  
526 which changes with distance and influences the magnitude and timing of the flood peak  
527 downstream. For example, W2080 has little difference in the shape of hydrograph (not  
528 surprising because of small change in CN) for the two LULC conditions, but its apparent  
529 change in UFR is very high because the time of the peak at its outlet is very different (big  
530 spread between the vertical lines in Fig 6.10). On the other hand, W2510 has a very different  
531 hydrograph, but because the peak at the outlet comes on the falling limb, and because there's  
532 a fairly small change in the time of the peak, the change in UFR is modest. Thus the effect of  
533 time matters more than the effect of changes in CN.

534



535 The characteristics of individual sub-catchments such as shape and slope may also play a  
536 vital role in the causal relationship between sub-catchment wise LULC changes and the flood  
537 peak at the basin outlet. These factors may partially explain why similar amounts of LULC  
538 change in different sub-catchments have varying impacts on the flood peak at the catchment  
539 outlets. It is likely that more than one of these factors are simultaneously playing a role in  
540 influencing the peak discharge at the catchment outlet. Thus, correcting the land use practice  
541 in one of the priority flood generating sub-catchments may not always result in reducing the  
542 flood peak. Hence, it is not surprising that this study did not find any pattern similar to one  
543 reported by Roughani et al. (2007), in which the sub-catchments located at the centroid of the  
544 catchment were found to be more likely to exert an influence to the peak discharge at the  
545 catchment outlet.

546

547 In order to implement remedial land management practices for controlling the flood peak at  
548 the reservoir inlet and reducing soil erosion, authorities like the DVC generally try to identify  
549 the sub-catchments that require urgent attention. If only a single LULC condition is of  
550 interest then the unit flood response approach (Saghafian and Khosroshahi, 2005) can be  
551 considered as an ideal solution to identify the priority target area for land-use planning.  
552 However, LULC conditions across sub-catchments change with time and the nature of this  
553 transformation from one LULC class to other LULC classes varies considerably from one  
554 sub-catchment to another. This factor tends to have a complex influence on the hydrologic  
555 response of the entire catchment over the years. Hence, the relevance of this study comes  
556 from testing whether local changes in LULC, at which scale the remedial measures are likely  
557 to be implemented, actually have a straight forward mitigating effect on the flood peak at the  
558 basin outlet. Pattison and Lane (2012) recommended that any empirical association found  
559 between local LULC change and downstream flood peak is valid only for that particular  
560 catchment and storm event. We suggest that, after identifying the major flood source areas  
561 for a storm event of approximately five year return period, further simulations should be carried  
562 out to evaluate the effect of possible remedial land-use planning in those sub-catchments over  
563 the flood peak at the cumulative basin outlet of interest. Undertaking remedial land-use  
564 measures in a few sub-catchments, especially in the upper catchment, may alter the tributary  
565 flow convergence timing in an adverse manner, nullifying the effects of corrective land  
566 management measures at the local scale.

567

568 Our study has emphasised the challenges faced in data scarce areas such as developing  
569 countries for modelling the impact of LULC changes on basin hydrology. The LULC maps  
570 were derived from freely available satellite data that varied in spatial and spectral resolution.  
571 In our study area, we had severe constraints in the availability of high-frequency (~hourly)  
572 rainfall data and historic ground truth data in terms of topographic maps, as well as low-cost,  
573 high resolution imagery such as Corona or GoogleEarth images. The reasonable match  
574 between the simulated and observed daily hydrographs for two rainfall events and LULC  
575 conditions demonstrated that the HEC-HMS model in conjunction with the NRSC CN  
576 method is capable of accurately reproducing rainfall-runoff processes with broad LULC  
577 classes and moderate resolution topography. Fig 5 and 6 illustrated that the HEC-HMS model  
578 setup in our study can accurately reproduce rainfall-runoff processes under two LULC  
579 conditions resulting from two different storm events. It established that the model can  
580 perform well independently of the nature of the storm event and LULC scenarios, and this  
581 provided an element of confidence when we applied the same storm event of 1973 for the  
582 LULC situations of 1976 and 2004 to address the core purpose of this research. Lower-  
583 frequency discharge data at the inlet of the Konar Reservoir might have hidden some  
584 mismatch between the observed and simulated surface runoff patterns. Availability of a more  
585 disaggregated observed streamflow record would have revealed some element of inaccuracies  
586 in the simulated hydrograph, possibly arising from the non-uniform distribution of actual  
587 rainfall depth, measurement errors in rainfall depth, coarse soil map and the low resolution of  
588 Landat MSS image (in terms of LULC and CN) or the SRTM DEM (in terms of delineation  
589 of channels, sub-catchments and channel configuration parameters for routing). In this  
590 context, we would like to highlight that availability of higher resolution LULC data would  
591 not make much difference in demonstrating the influence of LULC on the hydrological  
592 response, as Wang and Kalin (2011) reported that the selection of model parameters (derived  
593 from coarse quality inputs) had little influence on modelling the impact of changing LULC  
594 scenario on surface runoff with the NRSC CN method.

595

## 596 **6 Conclusion**

597

598 We have illustrated a systematic approach of analysing the effect of LULC changes in the  
599 sub-catchment level and their varying impact on the flood peak at the catchment outlet. An  
600 overall positive relationship was found between the two factors. However, our findings

601 indicated that varying timing of flow convergence between hillslope and streams at the sub-  
602 catchments caused by localised LULC changes is the key factor behind the frequent deviation  
603 from this overall trend. While unit flood response (Saghafian and Khosroshahi, 2005) is an  
604 innovative means of identifying the sub-catchments that need urgent attention in terms of  
605 land management to reduce flood peak, we argue that the complex interaction between  
606 changing LULC in sub-catchments, especially in large basins with heterogeneous LULC, is  
607 likely to be dependent on other factors which are not within the scope of this study. These  
608 factors may include soil types and nature and duration of the precipitation event. This study  
609 also demonstrated ways of utilising free or low-cost spatial and meteorological data, typically  
610 available in developing countries, to set up a widely used hydrological model that is capable  
611 of reproducing event scale rainfall-runoff processes with reasonable accuracy. The described  
612 methodology and the key findings will be beneficial for mitigating flooding through non-  
613 structural measures, particularly in the developing world.

614  
615  
616  
617  
618  
619  
620  
621  
622  
623  
624  
625  
626  
627  
628  
629  
630  
631  
632  
633  
634

## Acknowledgement

635  
636  
637  
638  
639  
640  
641  
642  
643  
644  
645  
646  
647  
648  
649  
650  
651  
652  
653  
654  
655  
656  
657  
658  
659  
660  
661  
662  
663  
664  
665  
666  
667  
668

We would like to thank Damodar Valley Corporation (DVC) for supplying the stream gauge records for the Konar River. Constructive review by the anonymous reviewer helped to improve the manuscript. Joy Sanyal was funded by a Durham Doctoral Fellowship.

669 **References**

670

671 Ali, M., Khan, S. J., Aslam, I., Khan, Z., 2011. Simulation of the impacts of land-use change  
672 on surface runoff of Lai Nullah Basin in Islamabad, Pakistan. *Landscape and Urban Planning*.  
673 102(4), 271-279.

674

675 Amini, A., Ali, T., Ghazali, A., Aziz, A., Akib, S., 2011. Impacts of Land-Use Change on  
676 Streamflows in the Damansara Watershed, Malaysia. *Arabian Journal for Science and*  
677 *Engineering*, 36(5), 713-720. doi 10.1007/s13369-011-0075-3

678 Amutha, R. and Porchelvan, P., 2009. Estimation of surface runoff in Malattar sub-watershed  
679 using SCS-CN method. *Journal of the Indian Society of Remote Sensing*. 37(2), 291-304.

680 Andréassian, V., 2004. Water and forests: from historical controversy to scientific  
681 debate. *Journal of Hydrology*. 29, 1–27.

682

683 Beighley, R.E. and Moglen, G.E., 2003. Adjusting measured peak discharges from an  
684 urbanizing watershed to reflect a stationary land use signal. *Water Resources Research*. 39(4),  
685 1093.

686

687 Beschta, R.L., Pyles, M.R., Skaugset, A.E., Surfleet, C.G., 2000. Peakflow responses to  
688 forest practices in the western Cascades of Oregon, USA. *Journal of Hydrology*. 233, 102–  
689 120.

690

691 Bhaduri, B., Harbor, J., Engel, B., Grove, M., 2000. Assessing watershed-scale, long term  
692 hydrologic impacts of land use change using a GIS-NPS model. *Environmental Management*.  
693 26(6), 643-658.

694

695 Bhattacharya, A. K., 1973. Flood control in the Damodar Valley. *Geographical Review of*  
696 *India*. 35(2), 134-146.

697

698 Bloschl, G., Ardoin-Bardin, S., Bonell, M., Dorninger, M., Goodrich, D., Gutknecht, D.,  
699 Matamoros, D., Merz, B., Shand, P., Szolgay, J., 2007. At what scale do climate variability  
700 and land cover change impact on flooding and low flows? *Hydrological Processes*. 21, 1241-  
701 1247.

702

703 Bosch, J.M. and Hewlett, J.D., 1982. A review of catchment experiments to determine  
704 the effect of vegetation changes on water yield and evapotranspiration. *Journal of*  
705 *Hydrology*. 55, 3–23.

706

707 Brink, A.B., and Eva, H.D., 2009. Monitoring 25 years of land cover change dynamics in  
708 Africa: A sample based remote sensing approach. *Applied Geography*. 29(4), 501-512.

709

710 Camorani, G., Castellarin, A., Brath, A., 2005. Effects of land use changes on the hydrologic  
711 response of reclamation systems. *Physics and Chemistry of the Earth*. 30, 561-574.

712

713 Candela, L., Tamoh, K., Olivares, G., Gomez, M. (2012) Modelling impacts of climate  
714 change on water resources in ungauged and data-scarce watersheds. Application to the  
715 Siurana catchment (NE Spain). *Science of The Total Environment*. 440, 253-260.

716  
717 Chen, Y., Xu, Y., Yin, Y., 2009. Impacts of land use change scenarios on storm-runoff  
718 generation in Xitiaoqi basin, China, *Quaternary International*. 208, 121-128.  
719 Choudhury, S., 2011. Damodar Valley Corporation, the missed opportunity. *Journal of*  
720 *Infrastructure Development*. 3(2), 117-126.  
721  
722 Collins, M.J., 2009. Evidence for changing flood risk in new England since the late 20th  
723 century. *J. Am. Water Resour. Assoc.* 45(2), 279–290.  
724  
725 Das, S.N., Narula, K.K., Laurin, R., 1992. Run-off potential indices of watersheds in Tilaya  
726 catchment, Bihar (India) through remote sensing and implementation of GIS. *Journal of*  
727 *Indian Society of Remote Sensing*. 20(4), 207-221.  
728  
729 Du, J., Qian, L., Rui, H., Zuo, T., Zheng, D., Xu, Y., Xu, C-Y., 2012. Assessing the effects of  
730 urbanization on annual runoff and flood events using an integrated hydrological modelling  
731 system for Qinhuai River basin, China. *Journal of Hydrology*. 464-465, 127-139.  
732  
733 Ewen, J., O'Donnell, G., Bulygina, N., Ballard, C., O'Connell, E., 2012. Towards  
734 understanding links between rural land management and the catchment flood hydrograph.  
735 *Q.J.R. Meteorol. Soc.* doi: 10.1002/qj.2026  
736  
737 Fox, D.M., Witz, E., Blanc, V., Soulié, C., Penalver-Navarro, M., Dervieux, A., 2012. A  
738 case study of land cover change (1950–2003) and runoff in a Mediterranean catchment.  
739 *Applied Geography*. 32(2), 810-821.  
740  
741 Ghosh, S., 2011. Hydrological changes and their impact on fluvial environment of the lower  
742 damodar basin over a period of fifty years of damming The Mighty Damodar River in  
743 Eastern India. *Procedia - Social and Behavioral Sciences*. 19, 511-519.  
744 DOI: 10.1016/j.sbspro.2011.05.163.  
745  
746 Hornbeck, J.W., Martin, C.W., Eagar, C., 1997. Summary of water yield experiments  
747 at Hubbard Brook Experimental Forest, New Hampshire. *Canadian Journal of Forest*  
748 *Research*. 27, 2043-2052.  
749  
750 Huffman, G.J., Adler, R.F., Bolvin, D.T., Gu, G., Nelkin, E.J., Bowman, K P., Hong, Y.,  
751 Stocker, E.F., Wolff, D.B., 2007. The TRMM multi-satellite precipitation analysis: Quasi-  
752 global, multi-year, combined-sensor precipitation estimates at fine scale. *Journal of*  
753 *Hydrometeorology*. 8, 38-55.  
754  
755 Hurkmans, R.T.W.L., Terink, W., Uijlenhoet, R., Moors, E.J., Troch, P.A., and Verburg, P.  
756 H., 2009. Effects of land use changes on streamflow generation in the Rhine basin. *Water*  
757 *Resources Research*. 45(6), W06405.  
758  
759 Jackson, T.J., Ragan, R.M., Fitch, W.N., 1977. Test of Landsat-based urban hydrologic  
760 modeling. *J. Water. Resour. Plann. Manag.* 103(1), 141–158.  
761  
762 Jia, H.J. and Wan, R.R., 2011. Simulating the impacts of land use/cover change on storm-  
763 runoff for a mesoscale watershed in east China. *Advanced Materials Research*. 347-353,  
764 3856-3862.

765 Knebl, M.R., Yang, Z.L., Hutchinson, K., Maidment, D.R., 2005. Regional scale flood  
766 modeling using NEXRAD rainfall, GIS, and HEC–HMS/RAS: a case study for the San  
767 Antonio River Basin Summer 2002 storm event. *Journal of Environmental Management*. 75,  
768 325–336.

769  
770 Kumar, P., Tiwari, K.N., Pal, D.K., 1991. Establishing SCS runoff curve number from IRS  
771 digital database. *Journal of the Indian Society of Remote Sensing*. 19 (4), 245-251.  
772

773 McColl, C. and Agget, G., 2007. Land use forecasting and hydrologic model integration for  
774 improved land use decision support. *Journal of Environmental Management*. 84, 494-512.  
775

776 Miller, W.P., 2002. Integrating landscape assessment and hydrologic modeling for land cover  
777 change analysis. *J American Water Resour Assoc*. 38(4), 915–929.  
778

779 Mishra, S.K. and Singh, V.P., 2003. *Soil Conservation Service Curve Number Methodology*.  
780 Kluwer Academic Publishers, Dordrecht, The Netherlands.  
781

782 Mishra, S.K., Pandey, R.P., Jain, M.K., Singh, V.P., 2008. A rain duration and modified  
783 AMC dependant SCS-CN procedure for long duration rainfall-runoff events. *Water*  
784 *Resources Management*. 22, 861-876.  
785

786 Natural Resources Conservation Service (NRCS), 1972. *National Engineering Handbook*,  
787 Section 4, Hydrology, U.S. Government Printing Office.  
788

789 O'Connell, E., Ewan, J., O'Donnell, G., Quinn, P., 2007. Is there a link between agricultural  
790 land use management and flood risk? *Hydrology and Earth System Sciences*. 11, 96-107.  
791

792 O'Donnell, G., Ewen, J., O'Connell, P.E., 2011. Sensitivity maps for impacts of land  
793 management on an extreme flood in the Hodder catchment, UK. *Physics and Chemistry of*  
794 *the Earth, Parts A/B/C*. 36 (13), 630-637.  
795

796 Olang, L.O. and Furst, J., 2011. Effects of land cover change on flood peak discharges and  
797 runoff volumes: model estimates for the Nyando River Basin, Kenya. *Hydrological Processes*.  
798 25, 80-89.  
799

800 Pattison, I., Lane S.N, Hardy, R.J., Reaney, S., 2008. Sub-catchment peak flow magnitude  
801 and timing effects on downstream flood risk. Paper presented at 10th National hydrology  
802 symposium, 15–17 September 2008 Exeter.  
803 <http://www.hydrology.org.uk/Publications/exeter/44.pdf> (Accessed on 30th October, 2013)  
804

805 Pattison, I. and Lane, S.N., 2012. The link between land-use management and fluvial flood  
806 risk: A chaotic conception? *Progress in Physical Geography*. 36(1), 72-92  
807

808 Rajeevan, M. and Bhate, J., 2008. A high resolution daily gridded rainfall data set (1971-  
809 2005) for mesoscale meteorological studies. National Climate Centre Research Report No:  
810 9/2008. National Climate Centre, Indian Meteorological Department, Pune, India.  
811 [http://www.imdpune.gov.in/ncc\\_rept/RESEARCH%20REPORT%209.pdf](http://www.imdpune.gov.in/ncc_rept/RESEARCH%20REPORT%209.pdf)  
812 (Accessed 30th October, 2013)  
813  
814

815 Roughani, M., Ghafouri, M., Tabatabaei, M., 2007. An innovative methodology for the  
816 prioritisation of sub-catchments for flood control. *International Journal of Applied Earth*  
817 *Observation and Geoinformation*. 9, 79-87.  
818

819 Saghafian, B. and Khosroshahi, M., 2005. Unit response approach for priority determination  
820 of flood source area. *Journal of Hydrologic Engineering*, 10 (4), 270-277.  
821

822 Saghafian, B., Farazjoo, H., Bozorgy, B., Yazdandoost, F., 2008. Flood intensification due to  
823 change in land use. *Water Resources Management*. 22, 1051-1067.  
824

825 Sanyal, J., Carbonneau, P., Densmore, A. L., 2013. Hydraulic routing of extreme floods in a  
826 large ungauged river and the estimation of associated uncertainties: A case study of the  
827 Damodar River, India. *Natural Hazards*. DOI: 10.1007/s11069-012-0540-7

828 Sanyal, J., Carbonneau, P., Densmore, A.L., (In Press). Low-cost open access flood  
829 inundation modelling with sparse data: A case study of the lower Damodar river basin, India.  
830 *Hydrological Sciences Journal*.

831 Sharma, K.D. and Singh, H., 1992. Runoff estimation using Landsat Thematic Mapper data  
832 and SCS model. *Hydrological Sciences Journal*. 37(1), 39-52.

833 Shi, P.J., Yuan, Y., Zheng, J., Wang, J.A., Gi, Y., Qiu, G.Y., 2007. The effect of land  
834 use/cover change on surface runoff in Shenzhen region, China. *Catena*, 69(1), 31-35.  
835

836 Slack, R.B. and Welch, R., 1980. SCS runoff curve number estimates from Landsat data.  
837 *Water Resour Bull.* 16(5), 887–893.  
838

839 Stuebe, M.M. and Johnston, D.M., 1990. Runoff volume estimation using GIS technique.  
840 *Water Resour Bull.* 26(4), 611–620.  
841

842 Tiwari, K.N., Kumar, P., Sebastian, M., Pal, D.K., 1991. Hydrologic modelling for runoff  
843 determination. *International Journal of Water Resources Development*. 7(3), 178-184.  
844

845 Tripathi, M.P., Panda, R.K., Pradhan, S., Sudhakar, S., 2002. Runoff modelling of a small  
846 watershed using satellite data and remote sensing. *Journal of the Indian Society of Remote*  
847 *Sensing*. 30, 39-52.  
848

849 Van Dijk, A.I.J.M., Van Noordwijk, M., Calder, I.R., Bruijnzeel, L.A., Schellekens, J.,  
850 Chappell, N.A., 2009. Forest–flood relation still tenuous–comment on ‘Global evidence that  
851 deforestation amplifies flood risk and severity in the developing world’, in: Bradshaw, C.J.A.,  
852 Sodi, N.S., Peh, K.S.-H., Brook, B.W.(Eds.), *Global Change Biol.* (15), 110–115.  
853

854 Wan, R. and Yang, G., 2007. Influence of Land use/cover change on storm runoff-A case  
855 study of Xitiaoxi River Basin in upstream of Taihu Lake watershed. *Chinese Geographical*  
856 *Science*. 17(4), 349-356.  
857

858 Wang, R. and Kalin, L., 2011. Modelling effects of land use/cover changes under limited data.  
859 *Ecohydrology*. 4, 265-276.  
860



861 Warburton, M.L., Schulze, R.E., Jewitt, G.P.W., 2012. Hydrological impacts of land use  
862 change in three diverse South African catchments. *Journal of Hydrology*. 414–415, 118-135.

863

864 Wei, X., Sun, G., Liu, S., Jiang, H., Zhou, G., Dai, L., 2008. The forest-streamflow  
865 relationship in China: a 40-year retrospect. *J. Am. Water Resour. Assoc.* 44 (5), 1076–1085.

866

867 Xu, Y., Xu, C., Gao, X., and Luo, Y., 2009. Projected changes in temperature and  
868 precipitation extremes over the Yangtze River Basin of China in the 21st century. *Quaternary*  
869 *International*. 208(1–2), 44–52.

870

871

872

873

874

875

876

877

878

879

880

881

882

883

884

885

886

887

888

889

890

891

892

893

894

895

896

897

898 **List of Tables:**

899 **Table 1** Percentage coverage of different LULC categories for 1976 and 2004 and the changes  
900 between the two time periods.

901		<b>LULC Classes</b>	<b>Percentage</b>	<b>Percentage</b>	<b>Difference in Percentage Cover</b>
902			<b>Cover 1976</b>	<b>Cover 2004</b>	<b>(2004 - 1976)</b>
903					
904	1.	Water body	5.4	5.9	0.5
905	2.	Rocky wasteland	9.7	24.2	14.5
906	3.	Urban	0.1	8.2	8.1
907	4.	Paddy Field	42.3	20.9	-21.4
908	5.	Shrub	9.6	23.2	13.6
909	6.	Open Forest	26.5	14.5	-12
910	7.	Dense Forest	11.3	8.2	-3.1

911

912

913

914

915

916

917

918

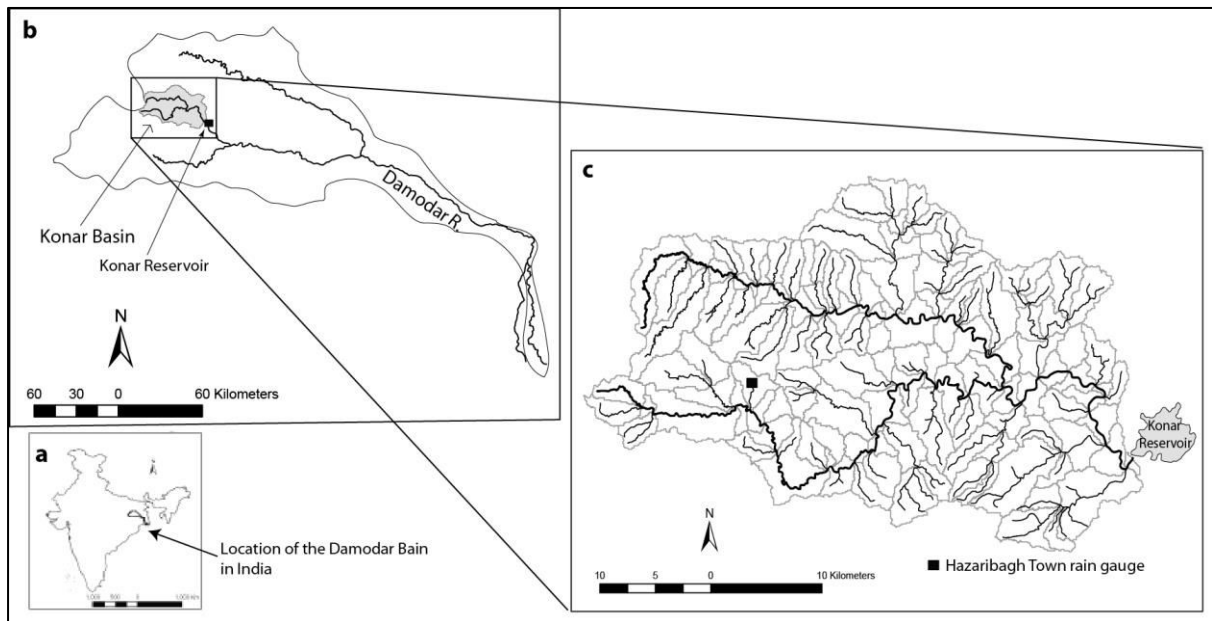


**Fig 1** The Study area; a: Location of the Damodar Basin In India, b: Location of the Konar River catchment in the Upper Damodar River Basin, c: The sub-catchments of the Konar River derived from the SRTM DEM with dark lines showing the streams vectorised from topographic maps. Automatically extracted drainage networks (derived from the SRTM DEM with a threshold contributing area of  $5 \text{ km}^2$ ) that approximately correspond with the 2nd order streams from the topographic maps were used to delineate the 124 sub-catchments.

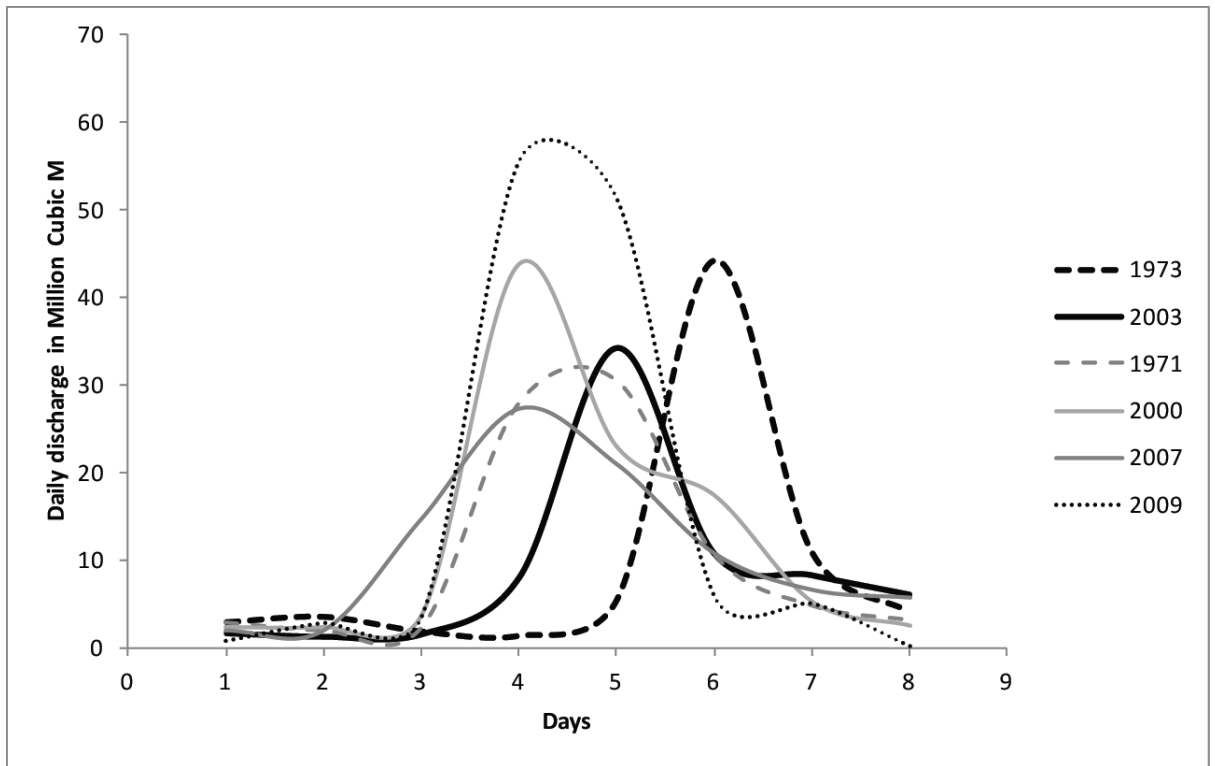


**Fig 2** Some major observed storm hydrographs in last four decades at the entry of Konar Reservoir. The storm events under consideration in this study (1973 and 2003) are shown in thick lines.

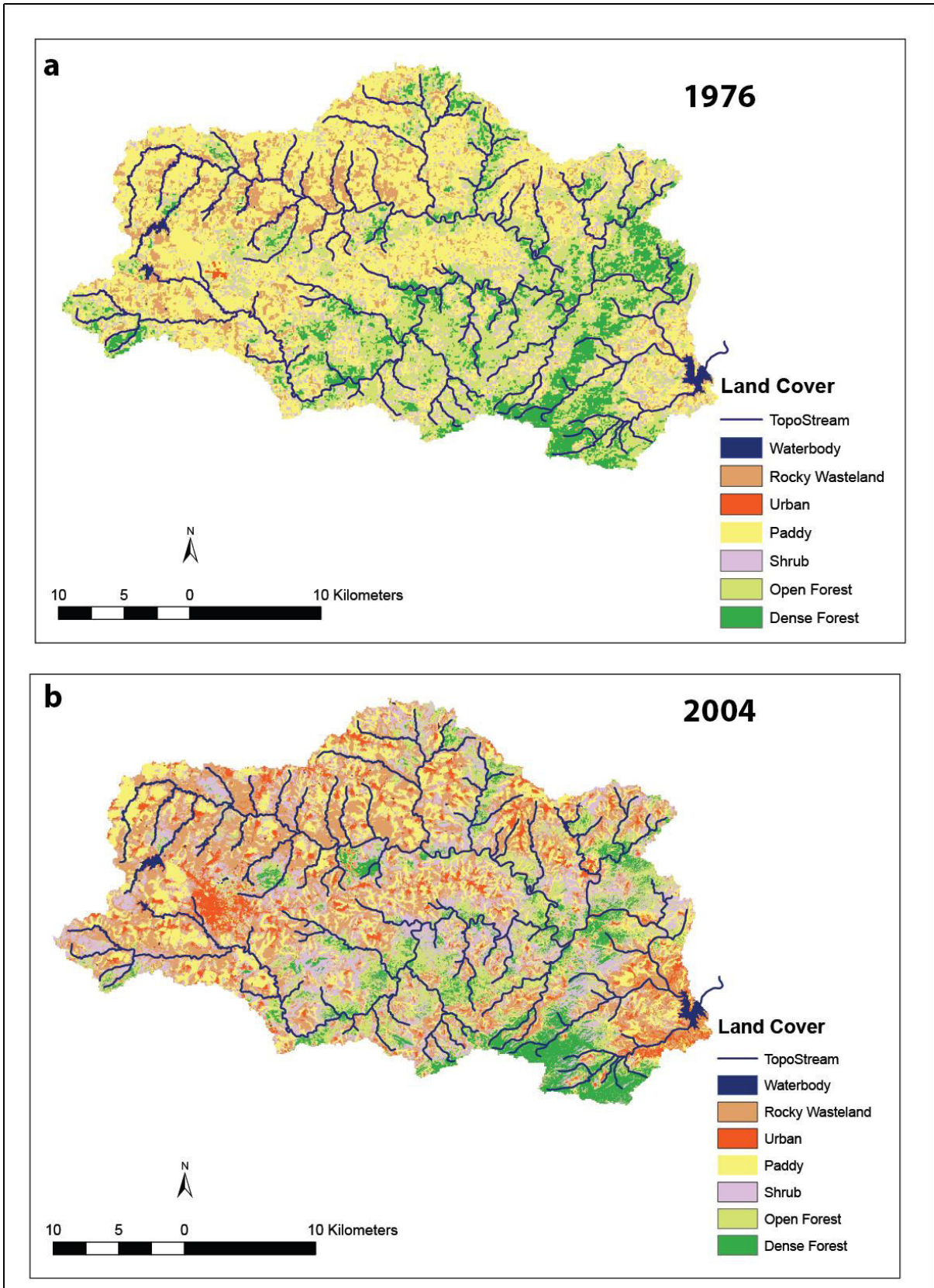


**Fig 3** Land cover classification of (a) 1976 and (b) 2004. Maps were derived from Landsat MSS (a) and Landsat TM (b) in the early post-monsoon season in late October to early November.

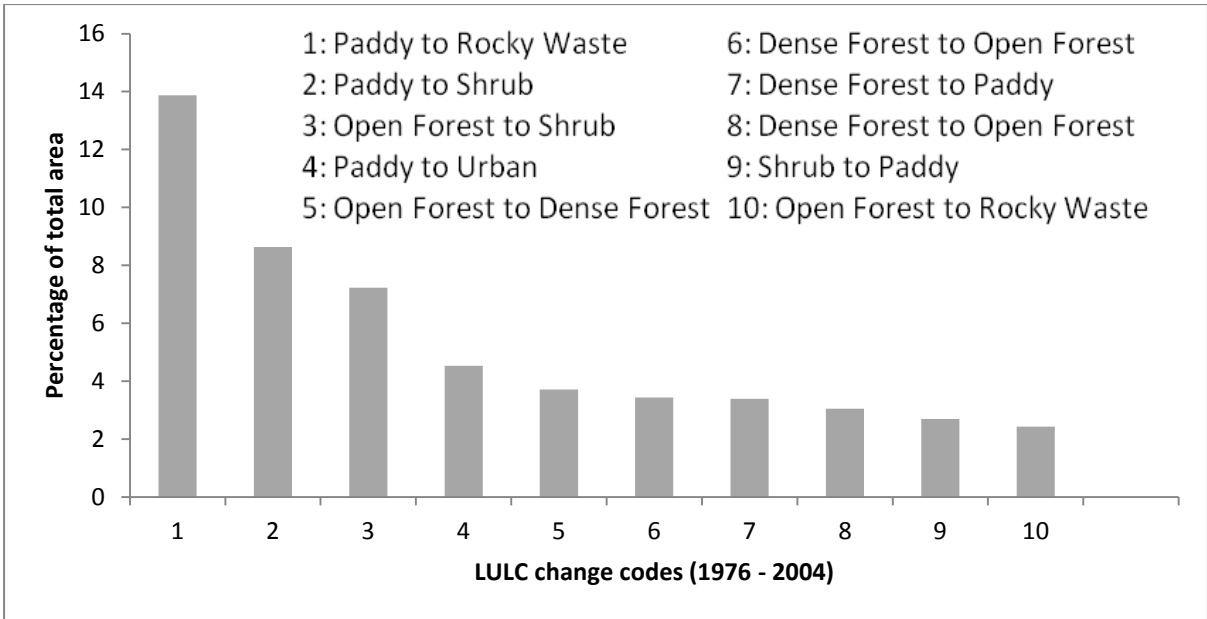


**Fig 4** Percentage of land in the Konar basin that had undergone substantial transformation from one LULC category to another between 1976 to 2004. These LULC scenarios are valid for the early post-monsoon season in late October to early November.

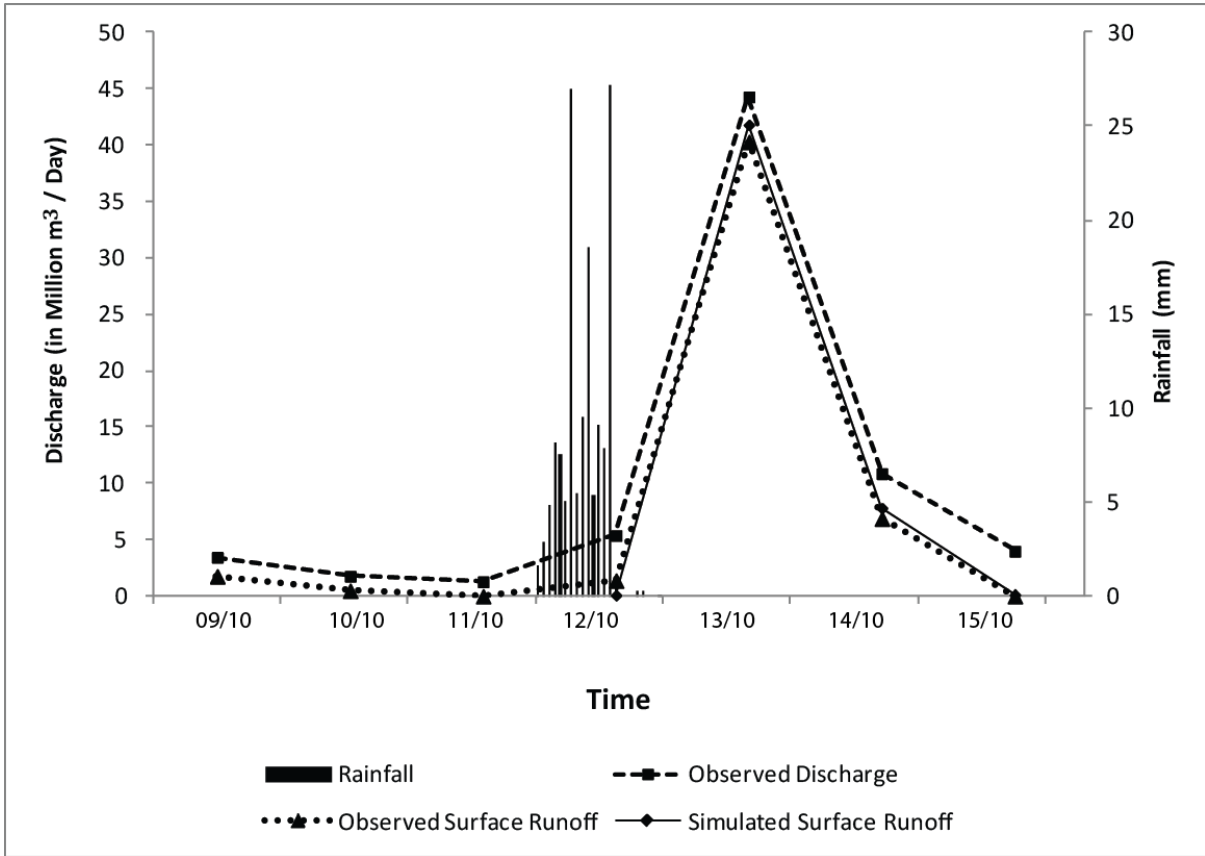


**Fig 5** Simulated surface runoff with gauged hourly rainfall input of October 1973 and land cover of 27th October, 1976. The observed surface runoff (depicted as dotted line) was derived from the observed discharge figure by means of base flow separation.

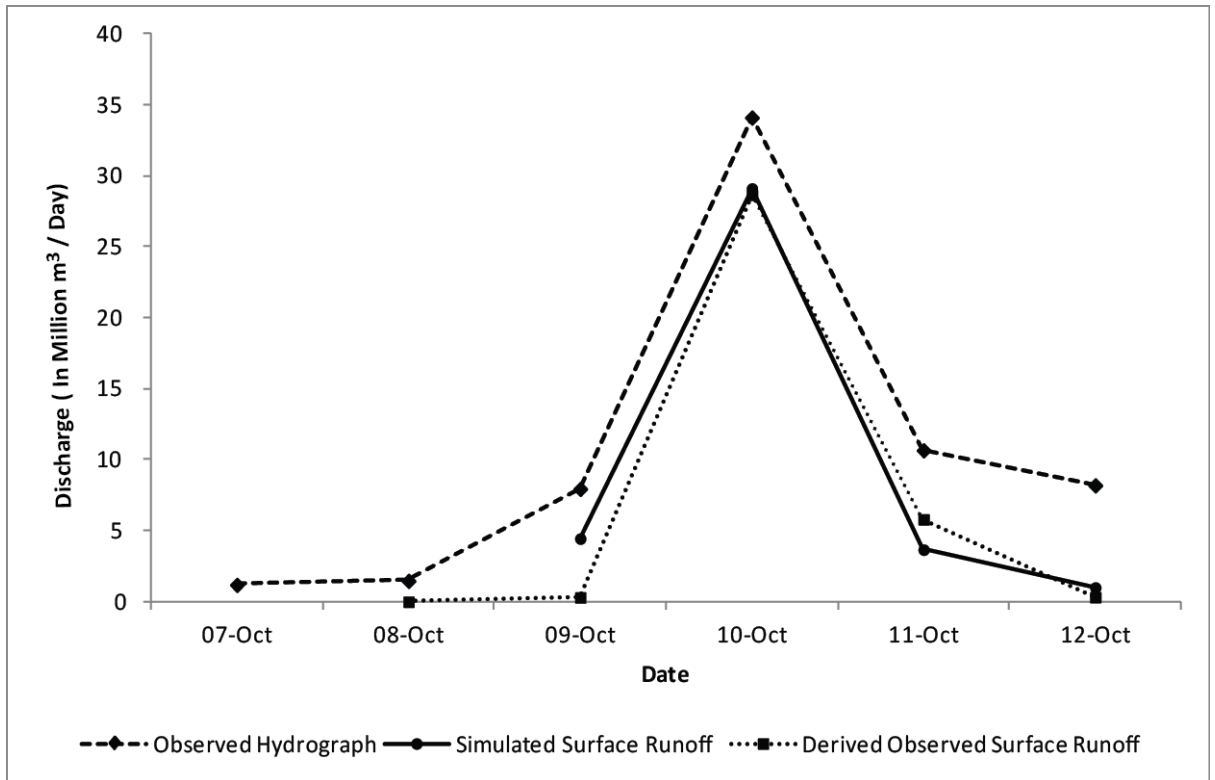


**Fig 6** Simulated surface runoff with TRMM 3-hourly rainfall input of October, 2003 and land cover of 2nd November, 2004.



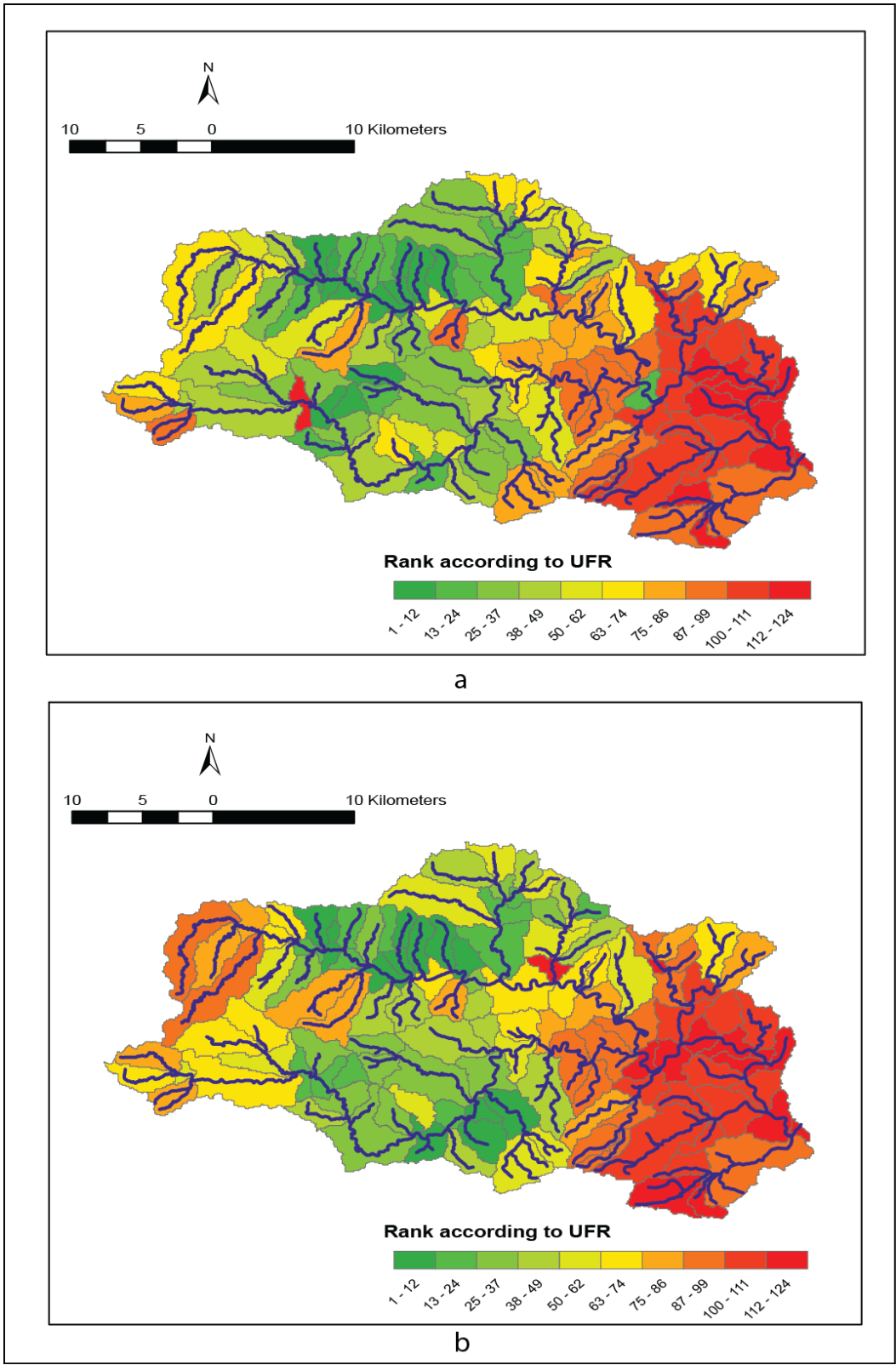


**Fig 7** Rank of the sub-catchments according to the unit flood response (UFR) values derived with the land cover of 1976 (a) and 2004 (b). The gauged hourly storm rainfall event of October, 1973 was used as the meteorological input in both models.

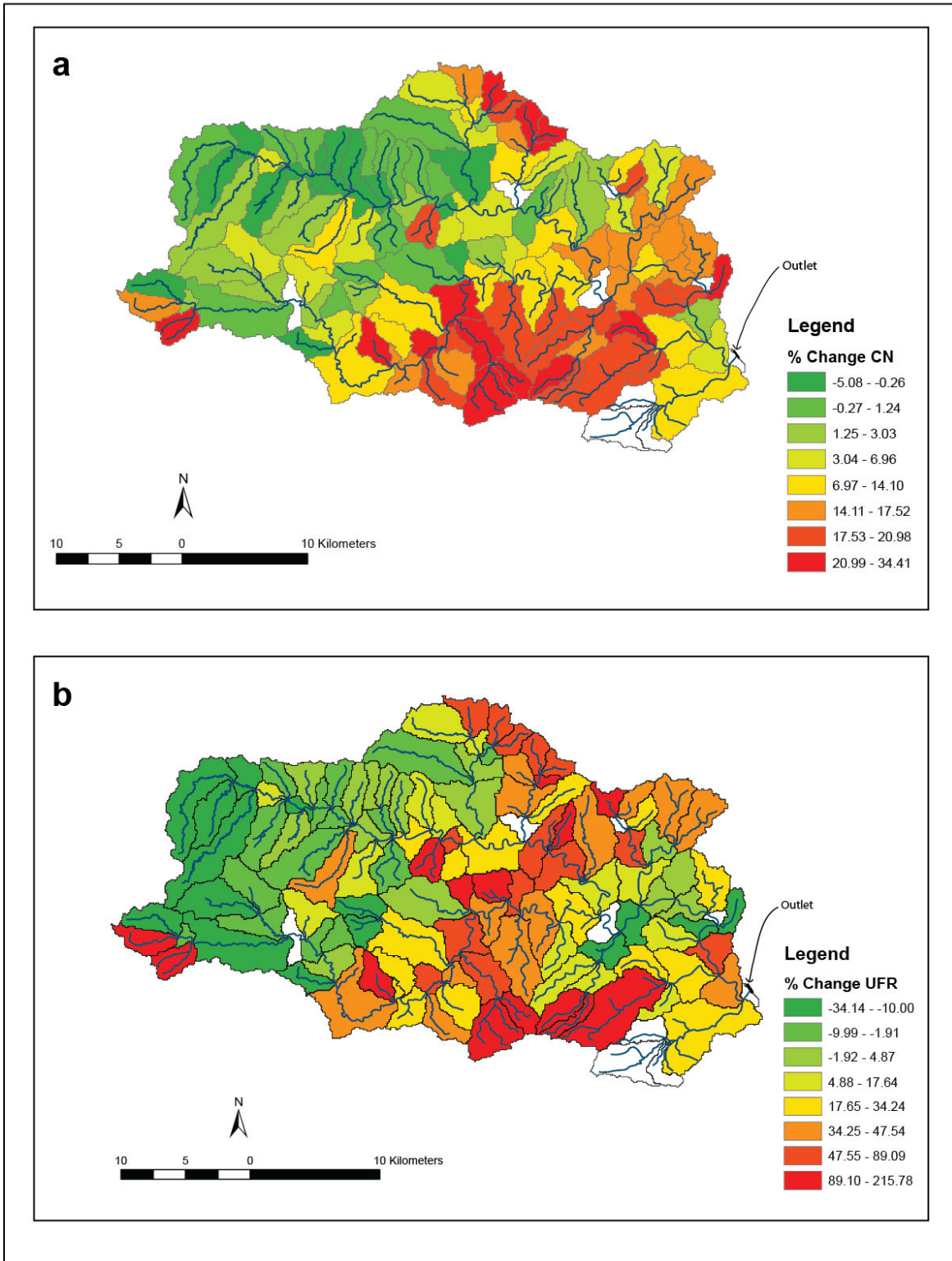


**Fig 8** a, percentage change in NRCS Curve Number (CN) values (1976 - 2004); b, percentage change in unit flood response (UFR) values (1976 land cover to 2004 land cover). In both panels, negative values indicate that the CN or UFR was higher in 1976 than 2004, and positive values show the opposite. The sub-catchments shown in white experienced negligible change. The class intervals of the data represented in Panel a and b have been derived from eight quantiles of the respective series.

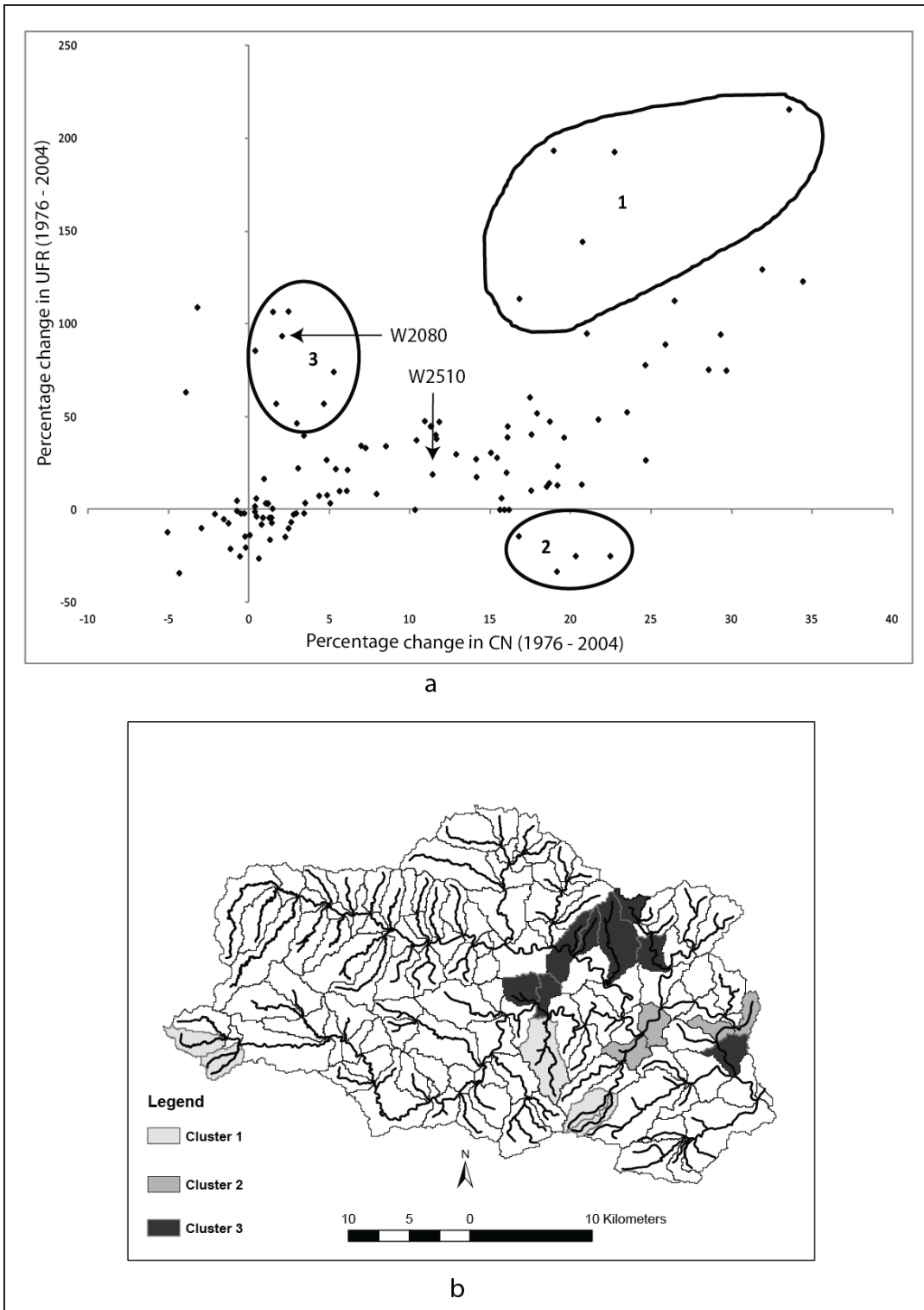


**Fig 9** a, Scatter diagram of the sub-catchment wise percentage changes in the unit flood response (1976 - 2004) and curve number (CN) values. Sub-catchments that did not fit into the overall linear positive correlation pattern were separated into 3 clusters. Sub-catchments W2080 and W2510 were selected as representative of extreme and typical cases, respectively, of UFR change in relation to changing LULC conditions. b, Location of the sub-catchments identified as 3 clusters in panel a.

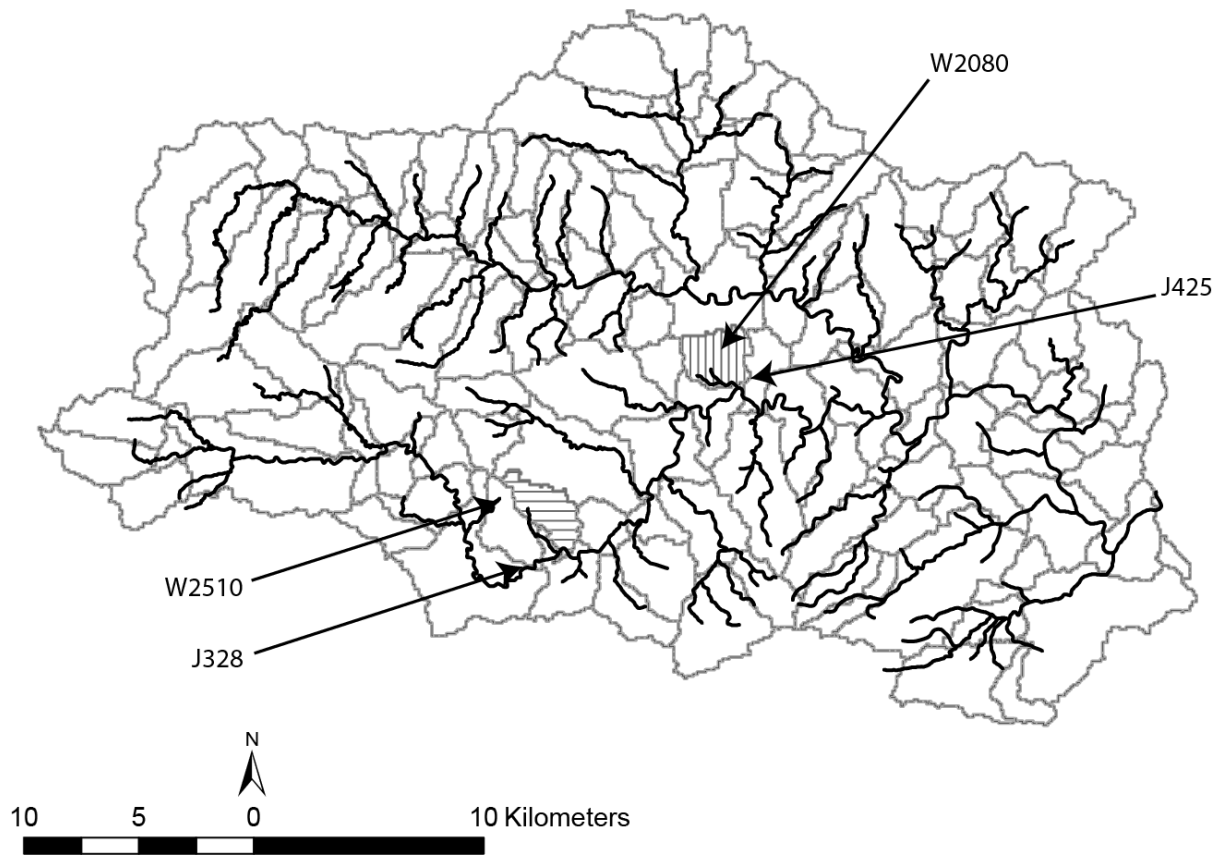


**Fig 10** Location of the sub-catchments and flow junctions that were selected for testing the influence of timing effects of flow convergence on the relationship of local LULC changes and downstream flood peak.

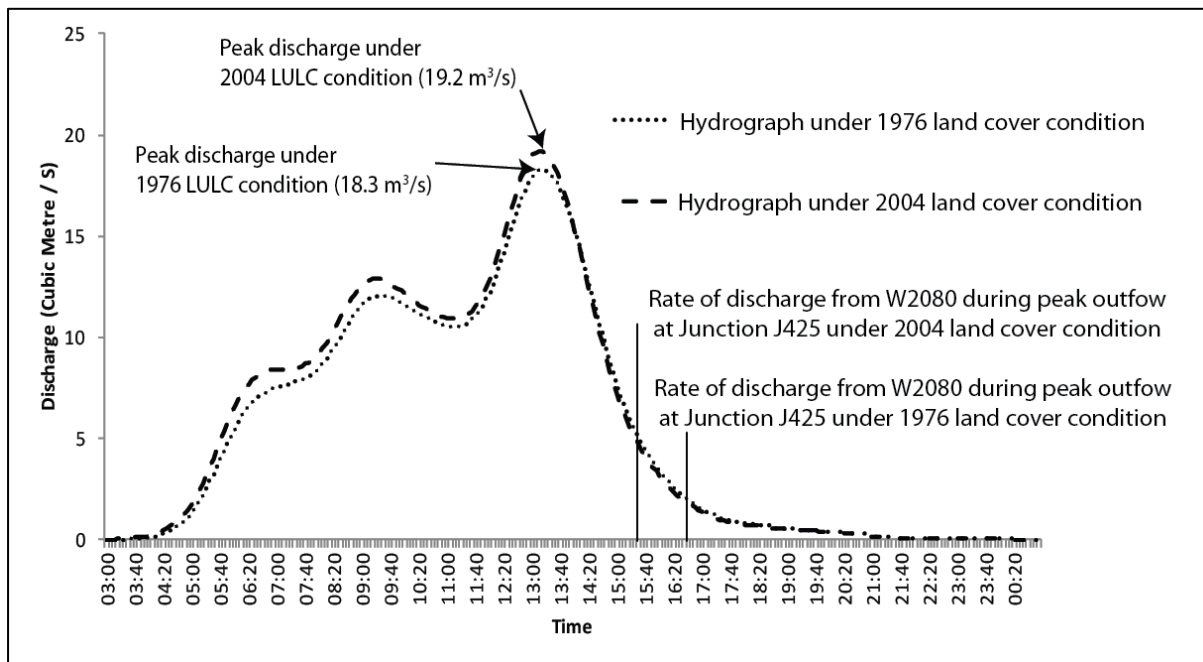


**Fig11** Hydrographs of sub-catchment W2080 for 1976 and 2004 LULC scenarios. Vertical lines show the timing of the combined peak flow at J425 for the 1976 and 2004 LULC.

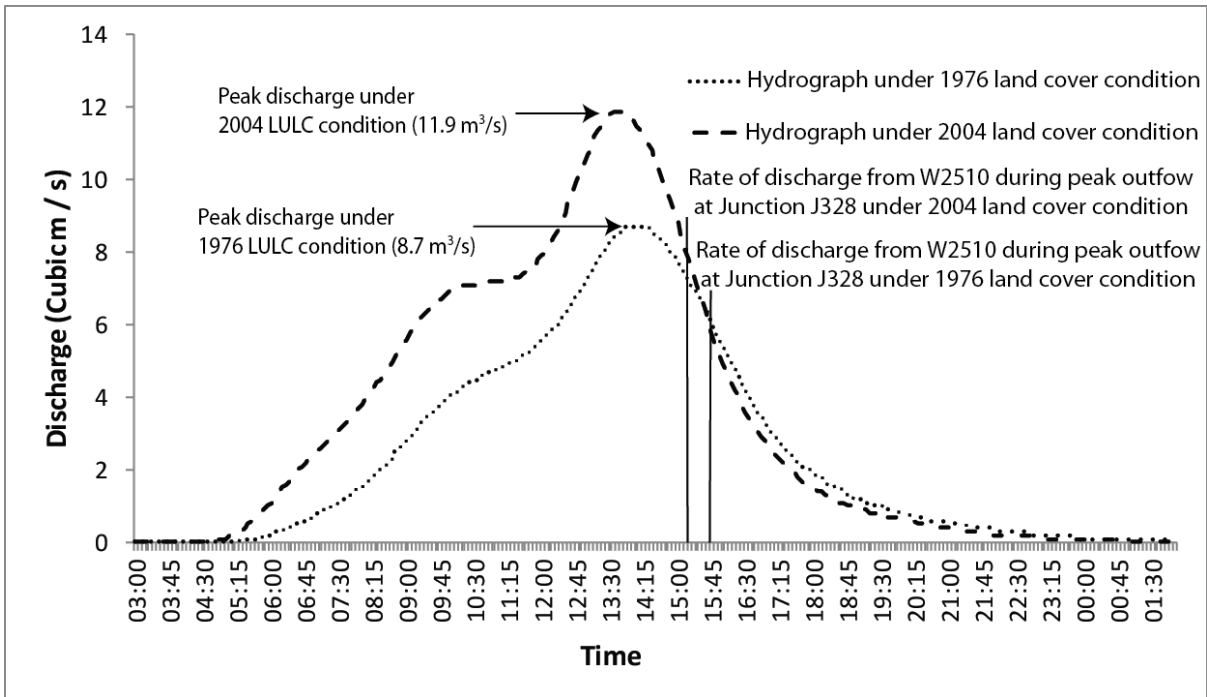


**Fig12** Hydrographs of sub-catchment W2510 for 1976 and 2004 LULC scenario, Vertical lines show the timing of the combined peak flow at J328 for the 1976 and 2004 LULC.